



Universiteit
Leiden
The Netherlands

Photothermal studies of single molecules and gold nanoparticles : vapor nanobubbles and conjugated polymers

Hou, L.

Citation

Hou, L. (2016, June 14). *Photothermal studies of single molecules and gold nanoparticles : vapor nanobubbles and conjugated polymers*. *Casimir PhD Series*. Retrieved from <https://hdl.handle.net/1887/40283>

Version: Not Applicable (or Unknown)

License: [Licence agreement concerning inclusion of doctoral thesis in the Institutional Repository of the University of Leiden](#)

Downloaded from: <https://hdl.handle.net/1887/40283>

Note: To cite this publication please use the final published version (if applicable).

Cover Page



Universiteit Leiden



The handle <http://hdl.handle.net/1887/40283> holds various files of this Leiden University dissertation.

Author: Hou, L.

Title: Photothermal studies of single molecules and gold nanoparticles : vapor nanobubbles and conjugated polymers

Issue Date: 2016-06-14

6

Simultaneous absorption and emission measurements of single conjugated polymers in near-critical xenon

***Abstract**– We simultaneously measure the absorption and emission of single conjugated polymers poly[2-methoxy-5-(2-ethylhexyloxy)-1,4-phenylenevinylene] (MEH-PPV) using supercritical xenon to enhance the photothermal contrast for direct absorption measurements. We obtain a number of useful pieces of information such as the number of monomers in single conjugated polymer molecules and the apparent quantum yield of single-polymer molecules. Simultaneous absorption and emission measurements provide new insight into the exciton behavior in a conjugated polymer molecule under optical excitation.*

6.1. Introduction

Conjugated polymers represent an important class of organic materials widely used in applications such as organic light emitting devices (OLED) [60], solar energy conversion [61], thin-film transistors and chemical sensors [63]. It is widely accepted that the optical and electrical properties strongly depend on the microscopic structure of conjugated polymers chains and on the local surroundings [119]. Over the past decades, with the help of single-molecule fluorescence spectroscopy [120], extensive studies have been carried out aiming to resolve the relationship between the optical properties of the conjugated polymers and their conformation [62]. Barbara's group first applied single-molecule spectroscopy to study single conjugated PPV-PPyV polymers in polystyrene [121]. Surprisingly, they found that a single conjugated polymer that consists of many chromophores behaves like a single emitter. After examining many factors, they concluded that efficient intrachain energy transfer and changes in the quantum yield account for the single-emitter behavior. Since then, many approaches based on single-molecule fluorescence spectroscopy have been proposed and applied to conjugated polymer studies. A common approach is to measure the fluorescence time traces of single polymer chains with different time resolutions [122, 123] and under different experimental conditions, such as different polymer structures, molecular weights, solvents, matrix, sample preparations [122, 124–126]. Another important approach is the fluorescent excitation and emission polarization anisotropy measurements on conjugated molecules, combined with computer simulations [119] to characterize the anisotropic conformation properties [127, 128]. Room temperature [129, 130] and low temperature single-molecule spectroscopy [124, 129, 131] can spectrally resolve the interaction between chromophores in a conjugated polymer, providing a picture of the landscape of energy transfer. Time-resolved measurements can give information on the fast dynamics of excitons during "on" and "off" states, and thus indirectly yield insight into the excitons' migration along a single chain and the population of localization domains [132, 133]. Fluorescence correlation spectroscopy (FCS) has been used to study the solvent effect on the conformation of conjugated polymers in solution [134, 135], and dynamics of excitons under variable excitation power [136]. Combining far-field and near-field microscopy, researchers proposed to measure the absorption ellipsoid of single conjugated polymers [137]. Providing a few nm spatial resolution, AFM can be exploited to resolve the fine structure of some conjugated polymer molecules [138].

Single-molecule fluorescence spectroscopy allows researchers to study the emission and photophysics of a single polymer in great detail. However, directly

probing the absorption and non-radiative decay of excitons is still challenging. Measurements of polarization anisotropy could provide some information on the absorption and orientation of single dipole molecules, but conjugated molecules usually do not absorb and emit as single dipoles and polarization anisotropic measurements might not directly link to the absorption and conformation properties. On the other hand, information on the non-radiative channels of excitons can provide more insight into the quenching and dark states of conjugated molecules, thus clarifying some points of the debates that have arisen in previous studies.

Photothermal microscopy is a very useful tool for probing the local energy dissipation. Spatial sensitivity has been shown down to a 2.5 nm gold nanoparticle [44] and a single dye molecule [45]. Conventional photothermal microscopy relies on high optical excitation powers to reach single-molecule sensitivity [45]. However, such high powers limit the kind of detectable molecules to those resisting photo-bleaching at high excitation powers. In this chapter, we simultaneously measure the absorption and emission of single MEH-PPV conjugated polymers embedded in a PMMA matrix with a reasonably low excitation power using supercritical xenon as the transducing medium for the photothermal microscope. Close to its critical point, xenon exhibits divergent refractive index change with temperature, which greatly enhances the photothermal contrast (see Chapter 5). This allows the simultaneous detection of absorption and emission at much lower power (so that photobleaching becomes less significant). Our results yield for the first time the number of monomers and apparent quantum yield of a single conjugated polymer, and provide valuable information on the radiative and non-radiative decays of excitons in a conjugated molecule.

6.2. Experimental details

6.2.1. Optical setup

Simultaneous absorption and fluorescence measurements were performed on a home-built inverted microscope. A continuous-wave (CW) laser with a wavelength of 488 nm is modulated by an acousto-optic modulator at 53 kHz, and used to excite the conjugated polymer molecules. A CW laser beam with a wavelength of 815 nm is spatially overlapped with the excitation/heating beam. The two beams are both expanded to fill the back aperture of an oil immersion objective (Olympus, 60 \times , NA=1.45) and are focused on the sample-substrate interface. The reflected probe beam is collected by a photodiode (Femto DHPCA-100-F), and the signal is demodulated by a lock-in amplifier (SR844, Stanford Research Systems). The demodulated voltage signal gives the photothermal contrast. The fluorescence signal of the polymer molecules is collected by a

single-photon-counting avalanche photodetector (SPCM-AQR-16, Perkin-Elmer), and a set of filters are used to remove the excitation and probe beams.

6.2.2. Sample preparation

Cover glasses are cleaned with acetone, ethanol and Milli-Q water, separately. Then they are cleaned with ozone to remove all possible organic contamination. MEH-PPV polymers (with average molecular weight M_n about 150-250 kDa) and PMMA (with molecular weight M_n about 996 kDa) were bought from Sigma-Aldrich, and molecules of large molecular weight are selected by gel permeation chromatography (GPC) with $M_n = 2$ MDa and polydispersity 1.11. The PMMA was cleaned by precipitation in order to get rid of impurities [139]. Then PMMA was dissolved in toluene with concentration of about 1% w/w. High molecular weight fractions of MEH-PPV are dissolved in toluene with concentrations from 10^{-5} to 10^{-4} g/L, and further diluted ten times with PMMA solution. Then the mixture solution was spin-coated on a clean cover glass to obtain a film about 40 nm thick. The cover glass coated with MEH-PPV/PMMA is glued to a home-built high-pressure cell, leaving a clear aperture of about 0.75 mm diameter which is used for optical access. The high pressure is applied to xenon gas through narrow steel tubes and controlled with an auxiliary device (see Appendix B). The temperature of the whole cell is also controlled with a feedback device. We vary the temperature and pressure of xenon close to its critical point to achieve optimal sensitivity, and we use small gold nanoparticles to calibrate the photothermal signal (see Figure 6.1).

6.3. Results and discussion

In order to find the optimal conditions for the photothermal detection of single polymer molecules in xenon, we set out our measurements on small gold nanoparticles (20 nm in diameter) in xenon under variable temperature and pressure. We varied the temperature and pressure of xenon cell and we found that the best conditions for the photothermal contrast arise when the pressure and temperature of the xenon cell are about 6.1 MPa and 288 K, respectively (see Chapter 5 for more details). Note that the optimal conditions may change a bit for different measurements, probably because the purity of xenon in the pressure cell may not be exactly the same every time, even though the cell is flushed with xenon before each measurement. Figure 6.1 shows the histogram of photothermal contrast of 20 nm gold nanoparticles in xenon under 488 nm heating when the pressure and temperature are optimized. The distribution originates from the size deviation from 20 nm and the shape deviation from a sphere [42]. The mean photothermal signal (with respect to the background)

of 12 particles is $109 \pm 26 \mu\text{V}$. This data will be used as calibration to deduce the absorption cross section of single conjugated polymers, since the absorption cross section of a gold nanosphere can be easily calculated using the Mie theory (for 20 nm gold sphere, the absorption cross section is about 175 nm^2 in xenon close to the critical point at 488 nm wavelength. Refractive index data ($n = 1.1379 \pm 0.0008$) are taken from ref.[113]).

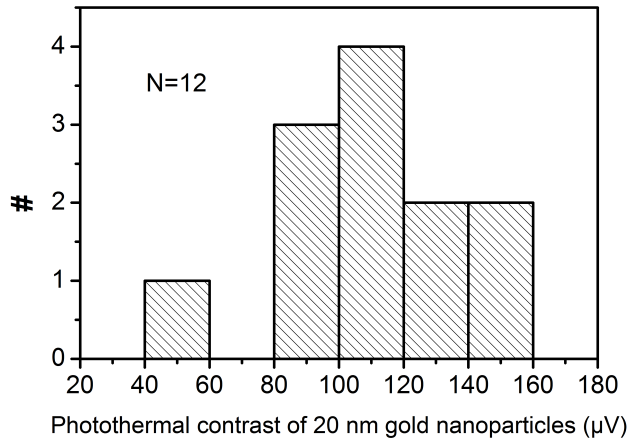


Figure 6.1: The histogram of the photothermal signal of 20 nm gold nanoparticles in near-critical xenon when the pressure and temperature are optimal (pressure is 6.1 MPa, temperature is 288 K). The heating power is $5 \mu\text{W}$ with a wavelength of 488 nm and linear polarization. The probe power is 15 mW at 815 nm. Powers are measured at the back focal plane of the objective (the objective transmission was not taken into account). Integration time is 10 ms, and heating modulation frequency is 53 kHz.

We simultaneously measured the absorption and emission of single MEH-PPV polymers embedded in PMMA using the enhanced photothermal setup. Typical confocal images are shown in Fig.6.2 (a) and (b). The excitation beam at 488 nm is circularly polarized in all the measurements discussed below. Single polymers show both fluorescence and absorption signals, and the big spots in both images are well correlated with each other. We scanned several different areas on the same sample, and we found 123 spots in the fluorescence image, 75 spots in the photothermal image and 60 correlated spots shown in both images. Some dimmer spots in the fluorescence image are not present in the photothermal image (one example is indicated by the dashed circles), probably because they have smaller molecular weight and low photothermal contrast which is beyond our current detection limit. Some spots that are present in the photothermal image do not show up in the fluorescence image, as shown in the dashed rectangular frame. This is possibly because of the photobleaching

6. Simultaneous absorption and emission measurements of single conjugated polymers in near-critical xenon

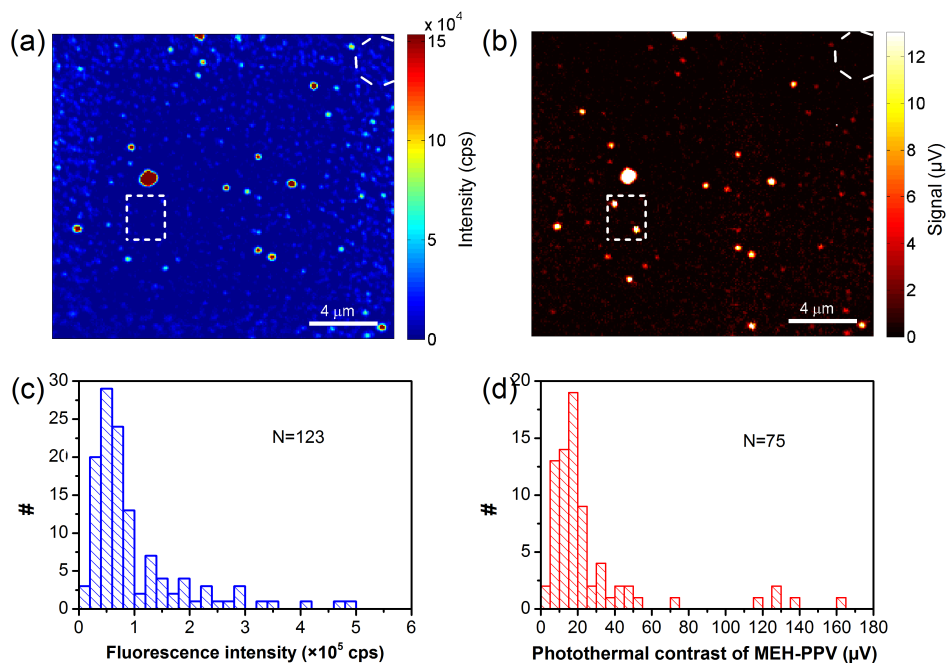


Figure 6.2: Simultaneous measurements of the emission and absorption of single MEH-PPV conjugated polymers under 488 nm excitation with circular polarization. a) confocal image of MEH-PPV's emission/fluorescence under $3.5 \mu\text{W}$ excitation power; b) simultaneous photothermal image of the same area. The heating power is $3.5 \mu\text{W}$, the probe power is 15 mW, integration time per pixel is 10 ms. The pressure and temperature of the xenon cell are 6.1 MPa and 289 K respectively. c,d) the histogram of fluorescence intensity c) and photothermal signal d).

of molecules during the laser scanning. The excitation/heating power used is approximately $3 \mu\text{W}$, corresponding to a power density of roughly 2 kW cm^{-2} (assuming the focused spot is diffraction-limited). The photothermal contrast of these polymer molecules is good enough, with average signal to noise ratio of about 55. We measured the two signals simultaneously on many spots, and plot the histograms of emission and absorption in Fig.6.2 (c) and (d). Both the emission and absorption show wide distributions probably due to the large molecular weight distribution and conformation heterogeneity, even though gel permeation chromatography (GPC) has been applied to sort out the polymers with relatively large molecular weight (see experimental details). Actually the molecular weight (MW) obtained from GPC does not truly reflect the molecular weight of the polymers in the matrix, as found and discussed in ref.[139]. This is because the concentration in these single-molecule experiments is much lower than that used in GPC, and the molecular weight of large conjugated

molecules is often overestimated in GPC due to the chain aggregation. The larger signals in the tail might be from some clusters and aggregates.

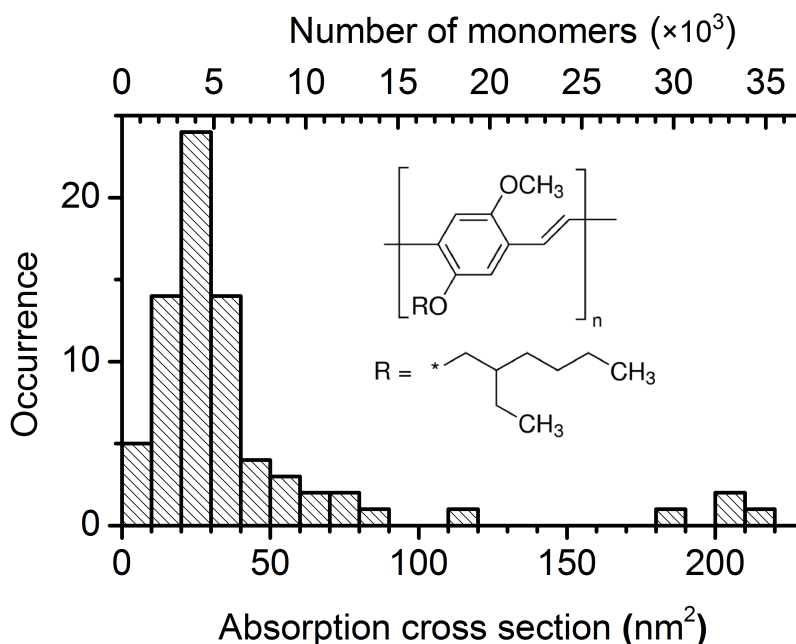


Figure 6.3: Estimation of the absorption cross section (lower axis) and the monomer numbers (top axis) of single MEH-PPV conjugated polymers in PMMA matrix based on the photothermal signal. Insert: chemical structure of the conjugated MEH-PPV molecule.

Now we can deduce the absorption cross section of a single polymer and the number of monomers in each polymer, based on the photothermal signal of polymer molecules and on the calibration data of 20 nm gold particles in Fig.6.1. Figure 6.3 shows the histogram of absorption cross sections of 75 polymer molecules. The mean value is about 40 nm² for the sample used. The wide distribution again reflects the size heterogeneity and/or aggregation of chains. Note that the histogram in Fig.6.3 may not fully reflect the distribution of the absorption cross section of these molecules because of the detection limit of current photothermal measurements. In order to have a reasonable photothermal signal, the SNR should not be smaller than 10 [42]. Then we estimate the minimum detectable absorption cross section to be around 8 nm² under current conditions. Since the absorption cross section of a monomer is about 6.2×10^{-3} nm² [140], the number of monomers in a single polymer molecule can be deduced from the absorption cross section, as shown on the top axis of Fig.6.3. The number of a few thousand monomers in a molecule is as ex-

pected from the sample preparation. To our best knowledge, our results are the first quantitative measurement of the monomer numbers in single conjugated polymers by photothermal microscopy. This useful information will help us to better estimate the quantum yield of a single polymer molecule.

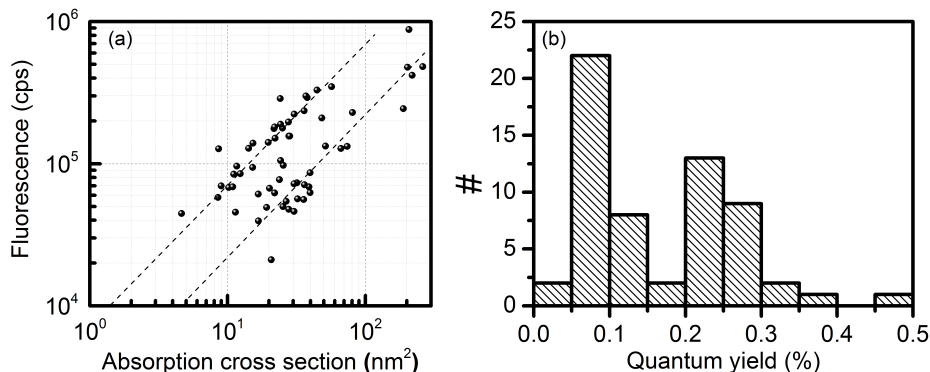


Figure 6.4: (a) Correlation plot of fluorescence brightness with absorption cross section. The dashed lines are guides for the eye with slope 1, where the data points are densely distributed. (b) Apparent quantum yield deduced from the correlated signals of (a).

With the knowledge of absorption and emission of a single conjugated polymer at hand, we can correlate these two signals and estimate the quantum yield of single polymers. In Fig.6.4 (a), we plot the fluorescent brightness as a function of the absorption cross section of polymer molecules. Each point represents a single polymer molecule that appears in both confocal images, 60 of them in the plot. There is a positive correlation between emission brightness and absorption cross section. The brighter the fluorescence is, the higher the absorption cross section of the polymer. The useful conclusion drawn here is that the brightness of fluorescence goes linearly with the number of monomers in a conjugated polymer molecule when the excitation power is low, as for our current measurements. Note that at high excitation powers, nonlinear behaviors of chromophores in a molecule such as singlet-singlet annihilation, singlet-triplet quenching and triplet-triplet annihilation will show up and become dominant. As the excitation power increases, fluorescence might get saturated or even decrease because of the build-up of long-lived triplet states and of increased possibilities of singlet-triplet quenching and singlet-singlet annihilation between chromophores [136, 141]. In the range of powers where these nonlinear effects take place, the dependence of the fluorescence on the number of monomers might not be linear any more. Additional measurements of the power dependence of both absorption and emission of polymer films and single molecules would be instructive to find out the linear power range. These

experiments are planned in the near future.

The quantum yield (QY) of an emitter is the ratio between the number of photons emitted and the number of photons absorbed under optical excitation, as written in Eq.6.1.

$$QY = \frac{N_{emit}}{N_{abs}}, \quad (6.1)$$

The total number of photons emitted N_{emit} in Eq.6.1 is the fluorescent signal divided by the detection efficiency of the setup (taking into account the transmission of all optics in the detection path and the efficiency of photon detectors), while the number of photons absorbed by a molecule N_{abs} is written as the ratio between absorbed power and incident photon energy:

$$N_{emit} = \frac{N_{fluo}}{\eta_{det}}, \quad (6.2)$$

$$N_{abs} = \frac{\sigma_{abs} I_{exc}}{h\nu_{exc}}, \quad (6.3)$$

where N_{fluo} is the measured fluorescence signal from a conjugated polymer molecule (counts per second); η_{det} is the detection efficiency of our current setup, and is estimated to be about 5% [141]; σ_{abs} is the absorption cross section of a single polymer molecule, deduced from the photothermal signal; I_{exc} and ν_{exc} are the excitation intensity at 488 nm and excitation frequency; h is the Planck constant.

In Fig.6.4 (b), we plot the histogram of apparent quantum yields for 60 molecules under 488 nm excitation. From the plot, two pieces of information are clearly visible. First, the distribution shows two peaks, possibly because two conformations dominate in the measured sample; Second, the quantum yields of these conjugated molecules are pretty low, a fraction of one percent, implying that there could be many "dark states" and non-radiative channels in the molecules under study. Greenham *et al.* [142] measured the absolute photoluminescence (PL) quantum efficiency of several conjugated polymers films, and the PL efficiency of MEH-PPV films is found to be in the range of $(0.1-0.15) \pm 0.01$ under 488 nm excitation, and efficiency decreases with time under ambient laboratory conditions. The storage condition could account for the low quantum yield we find since our spin-coated samples were stored under ambient conditions and measured several days after preparation. Lin *et al.* [143] have shown that for larger molecular weight MEH-PPV polymers, the fluorescence yield of individual molecules decreases, and the exciton's funneling model is not fully appropriate for these bigger molecules since a large fraction of the polymer chains are the "dark" regions. They do absorb light, but they do not participate in the radiative emission. This could be one of the reasons

6. Simultaneous absorption and emission measurements of single conjugated polymers in near-critical xenon

for the low quantum yield we find from the simultaneous measurements. Excitation power could also play a role in the quantum yield measurement, as observed in the study of organic dye nanoparticles in ref.[141]. At high excitation rate, strong interactions between singlet and triplet excitons among chromophores in a molecule can cause severe singlet-triplet quenching, singlet-singlet and triplet-triplet annihilations of excitons. As a consequence, the fluorescence and the apparent quantum yield will decrease in response to high excitation powers.

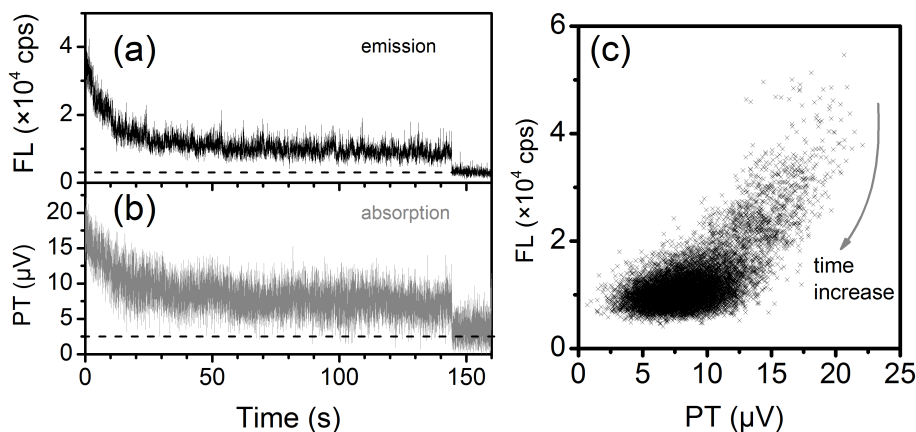


Figure 6.5: Transient traces of absorption and emission of a conjugated polymer molecule measured simultaneously. (a) fluorescence (FL) of the molecule; (b) photothermal signal (PT) of the same molecule measured simultaneously; (c) scatter plot of FL and PT showing different decay rates. The curved arrow indicates the time. The excitation power is about $3 \mu\text{W}$, the probe power is 15 mW and the integration time is 10 ms . The pressure and temperature of the xenon cell in the measurement is about 6.3 MPa and 288 K . The black dashed lines are the background levels. At about 140 s , the sharp step is because the focuses are manually shifted to a region where there are no molecules in order to record the background.

We can also have a look at the simultaneous transient traces of absorption and emission from individual polymer molecules. We did our measurements in the following sequence: first we image the polymer samples in the field of view with low excitation power (typically below $1 \mu\text{W}$ at the entrance of objective), and check single molecules by recording the transient blinking trace of fluorescence at low power. Then we go to slightly higher excitation power to record the simultaneous signals in absorption and emission while keeping the rate of photo-bleaching as low as possible. Under continuous illumination, we observed that most molecules in our current samples show continuous decrease simultaneously in both signals within a few seconds with different decay rates, as shown in Fig.6.5. The correlated continuous decays in both signals may re-

sult from the continuous bleaching of monomer absorbers. Two types of fluorescence signals have been extensively reported in many papers [122, 127, 144], and are attributed to the conformational heterogeneity of conjugated polymers in the host matrix. i) For the first type of polymer fluorescence, big polymer molecules behave like fluorescent beads. They tend to have extended conformations. There is no energy transfer or funneling between the chromophores, they absorb and emit photons independently. In this case, the time traces normally show an exponential decay of the fluorescence brightness with illumination time. ii) The second type of conjugated polymer fluorescence is attributed to collapsed conformations leading to strong intrachain interactions. Excitons created upon photon absorption by the chromophores can now migrate along the conjugated chain, and relax towards low-energy traps due to the "funneling" effect. In this second case emission mostly takes place from a few low-energy sites [121]. At high excitation power, singlet-triplet quenching, singlet to singlet and triplet to triplet annihilation are also expected to be more efficient in limiting the fluorescence [136]. The decays shown in Fig.6.5 seem to point to the first kind, with extended conformations. Yet, at this stage, we lack sufficient statistics for a reliable analysis of the decays of fluorescence and absorption. Further experiments need to be done to investigate this in more detail.

6.4. Conclusions and outlook

We measured the absorption and emission of individual conjugated MEH-PPV polymers simultaneously with an improved photothermal setup. We showed for the first time direct measurements of the absorption cross sections, the number of monomers and the apparent quantum yield of single conjugated polymer molecules. The quantum yield of the current samples is quite low and widely distributed. The conformation of conjugated polymers is closely related to their molecular weight, the polarity of the solvents used and the properties of the host matrix. Future simultaneous measurement on the absorption and emission will provide more insight into how these factors influence the optical properties of single conjugated polymer molecules.

6.5. Acknowledgments

We would like to acknowledge Dr. Yuxi Tian and Prof. Ivan Scheblykin for their efforts in making all the polymer samples used in this chapter and for helpful discussions about polymer properties. Advice from Dr. Subhasis Adhikari on polymer measurements are also kindly acknowledged. Mr Harmen van der Meer and guest Ms Tina Ding built the pressure cell used in the measurements. We gratefully acknowledge their support.

